Inorganic Chemistry

Article

pubs.acs.org/IC

Systematic Study of Cr^{3+} Substitution into Octahedra-Based Microporous Aluminoborates

Qiaoqi Li,[†] Cong Lin,[†] Zhengyang Zhou,[†] Jing Ju,[‡] Guobao Li,[‡] Jianhua Lin,[‡] Wenliang Gao,[†] Rihong Cong,*[,†] and Tao Yang*[,†]

[†]College of Chemistry and Chemical Engineering, Chongqing University, Chongqing 400044, People's Republic of China

[‡]Beijing National Laboratory for Molecular Science, State Key Laboratory of Rare Earth Materials Chemistry and Applications, College of Chemistry and Molecular Engineering, Peking University, Beijing, Hebei 100871, People's Republic of China

Supporting Information

ABSTRACT: Single crystals of pure aluminoborate PKU-1 ($Al_3B_6O_{11}(OH)_5{\cdot}nH_2O$) were obtained, and the structure was redetermined by X-ray diffraction. There are three independent Al atoms in the *R*3 structure model, and Al3 locates in a quite distorted octahedral environment, which was evidenced by ^{27}Al NMR results. This distortion of $Al3O_6$ octahedra release the strong static stress of the main framework and leads to a symmetry lowering from the previously reported $R\bar{3}$ to the presently reported *R*3. We applied a pretreatment to prepare Al^{3+}/Cr^{3+} aqueous solutions; as a consecquence, a very high Cr^{3+}-to-Al^{3+} substitution content (~50 atom %) in PKU-1 can be achieved, which is far more than enough for catalytic purposes. Additionally, the preference for Cr^{3+} substitution at the Al1 and Al2 sites was observed in the Rietveld refinements of the powder X-ray data of PKU-1:0.32Cr^{3+}. We also systematically investigated the thermal behaviors of PKU-1:$x$$Cr^{3+}$ ($0 \le x \le 0.50$) by thermogravimetric−differential scanning calorimetry, in situ high-temperature XRD in vacuum, and postannealing experiments in furnace. The main framework of Cr^{3+}-substituted PKU-1 could be partially retained at 1100 °C in vacuum. When $0.04 \le x \le 0.20$, PKU-1:$x$$Cr^{3+}$ transferred to the PKU-5:$x$$Cr^{3+}$ ($Al_4B_6O_{15}$:$x$$Cr^{3+}$) structure at ~750 °C by a 5 h annealing in air. Further elevating the temperature led to a decomposition into the mullite phase, $Al_4B_2O_9$:$x$$Cr^{3+}$. For $x > 0.20$ in PKU-1:$x$$Cr^{3+}$, the heat treatment led to a composite of Cr^{3+}-substituted PKU-5 and Cr_2O_3, so the doping upper limit of Cr^{3+} in PKU-5 structure is around 20 atom %.

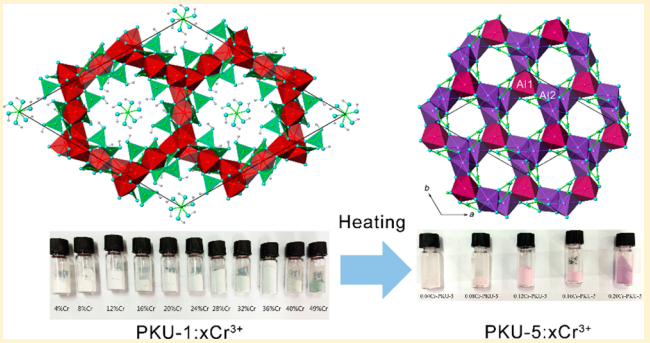

INTRODUCTION

The transition metal substitution into a microporous structure has a technological importance in catalysis. However, for traditional catalysts like zeolites, which possess tetrahedron-based frameworks, such an incorporation is quite difficult due to the strong preference of octahedral coordination for first-row transition metal ions. Therefore, high-concentration doping in tetrahedral-based structures would cause a significant structural distortion and thus easy catalytic deactivation. From this aspect, octahedra-based microporous materials have their advantage; however, such materials are rare, for example, the todorokite family (manganese oxide minerals),[1−3] wightmanite ($Mg_5O(OH)_5BO_3$),[4] VSB-5,[5] and PKU-*n* aluminoborates (PKU-1, PKU-2, and PKU-5).[6−8]

PKU-1, with the formula of $HAl_3B_6O_{12}(OH)_4{\cdot}nH_2O$, was first obtained by using the boric acid flux method.[6] The structure was originally solved by powder X-ray diffraction (XRD) in the trigonal space group $R\bar{3}$ (a = 22.0381(2) Å and c = 7.0261(1) Å). Al^{3+} ions are exclusively in octahedral coordination, and AlO_6 octahedra further share edges to form a three-dimensional porous framework with interpenetrated 18- and 10-membered channels. Borate species, in the forms of $BO(OH)_2$, $BO_2(OH)$, and $B_2O_4(OH)$, attach to the AlO_6-framework by sharing vertex oxygen atoms of AlO_6. Considerable residual electron densities within the 18-ring channels were detected by XRD, which had been originally identified as disengaged water molecules.

PKU-5 ($Al_4B_6O_{15}$) also possesses a pure AlO_6 octahedra-based framework, which shows a very high thermal stability.[7] Its structure was also determined by powder XRD, which crystallizes in *R*3 with the lattice constants of a = 11.433 98(9) Å and c = 6.483 07(5) Å. Its framework structure has a close relationship with PKU-1, indicated by the fact that PKU-5 can be obtained by thermal decomposition of Cr-incorporated PKU-1.

Other than the PKU-*n* family, there are growing studies on aluminoborates consisting of organic components or large polyborate clusters. For example, QD-2 ($[CH_3NH_2(CH_2)_3NH_3][AlB_5O_{10}]$) and QD-3 ($(TETA)_2[Al_2B_{10}O_{20}]{\cdot}0.25H_2O$) are two interesting aluminoborates, which both contain intersecting three-dimensional channels;[9,10] $[C_5H_6N]$-

Received: February 12, 2014
Published: May 20, 2014

   dx.doi.org/10.1021/ic500352g | *Inorg. Chem.* 2014, 53, 5600−5608

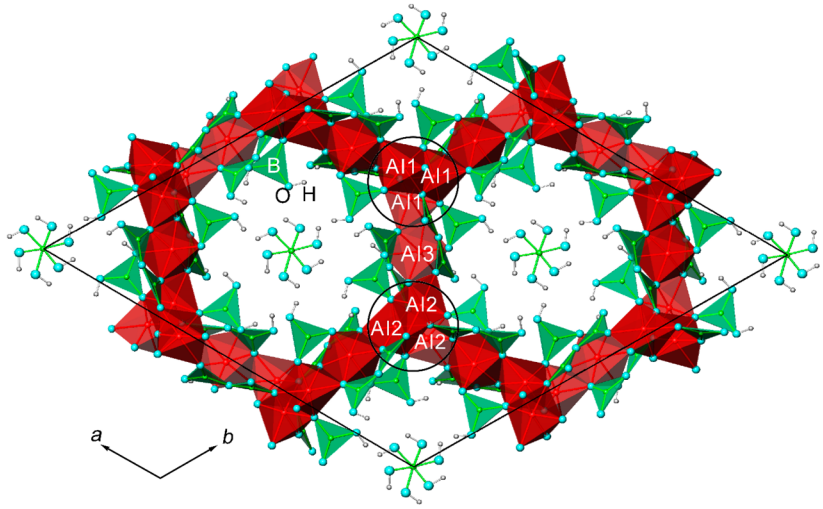

Figure 1. Structure of PKU-1 viewed along the *c* axis. Color code: red octahedra, AlO_6; green triangles, BO_3. Green, cyan, and gray spheres represent boron, oxygen, and hydrogen, respectively. Hydrogen bonds are shown as gray lines. The helix octahedra chains consisting of edge-shared $Al1O_6$ (and $Al2O_6$) are highlighted.

$[AlB_{12}O_{14}(OH)_{12}]$ and $Na_5[AlB_{24}O_{34}(OH)_{12}]\cdot nH_2O$ represent two cases of large polyborate clusters, where small hexaborate fragments are assembled by Al^{3+}.[11,12] In addition, there are several unusual aluminoborates synthesized by employing metal complexes as the structure-directing agents, for instance, $[M(dien)_2][(AlB_5O_9)(BO_2(OH)]$ (M = Co, Ni, Cd, Zn),[13] $[Zn(dien)_2][(Al(OH)(B_5O_9F)]$,[14] and $[In(dien)_2]$-$[Al_2B_7O_{16}H_2]$.[15]

We are particularly interested with aluminoborates because B and Al probably can serve as Lewis acid sites. Indeed, PKU-1 was recently proved to be a solid acid catalyst showing an activity to phenol hydrogenation with Pd-loading.[16] PKU-2 ($Al_2B_5O_9(OH)_3\cdot nH_2O$), which possesses 24-membered structural channels, shows an excellent catalytic activity to the cyanosilylation reaction of aldehydes under mild conditions.[8] A preliminary redox catalytic study was performed on Cr-substituted PKU-1, where Cr^{3+} was proved to be the active centers by the selective oxidation of styrene under mild reaction conditions.[17] Therefore, the Cr^{3+}-to-Al^{3+} substituted PKU-*n* alminoborates may serve as bifunctional catalysts. It was mentioned in literature that Cr^{3+} could be successfully doped into PKU-*n* alminoborates, but without details. As a consequence, it becomes necessary and urgent to systematically investigate the substitution behavior of Cr^{3+} into octahedra-based aluminoborates PKU-1 and PKU-5.

First, we improved the synthesis strategy and obtained needle-like single crystals of PKU-1. Then the structure was redetermined by single-crystal XRD, which confirmed the previously reported main framework but with a lower symmetry in the space group *R*3. Furthermore, the upper limit of Cr^{3+} doping into the framework of PKU-1 is significant, ~50 atom %. We investigated the thermal behaviors of PKU-1:*x*Cr^{3+} by thermogravimetric analysis−differential scanning calorimetry (TGA-DSC), in situ high-temperature XRD in vacuum, and annealing experiments in furnace. Accordingly, an enhancement of the thermal stability of the PKU-1 structure by the incorporation of Cr^{3+} was observed; for instance, the framework of PKU-1:0.10Cr^{3+} can be partially retained at 1000 °C in vacuum. Additionally, the appropriate annealing conditions for obtaining PKU-5:*x*Cr^{3+} from PKU-1 were also studied.

EXPERIMENTAL SECTION

Syntheses. *Crystal Growth of PKU-1.* The synthesis was carried out in a closed Teflon autoclave by the boric acid flux method. We performed a prereaction process on the aluminum source. $Al(NO_3)_3\cdot 9H_2O$ (5 mmol) and 0.5 mL of concentrated HNO_3 were charged to a 25 mL Teflon container, which was sealed and heated at 80 °C for 5 h. After the container was cooled, 150 mmol of H_3BO_3 was added, and the vessel was sealed again with a stainless steel shell. It was heated slowly to 220 °C in an oven and kept for 7 d. The products were washed with water until the excess boric acid was completely removed; then they were dried at 80 °C for further characterization. Sharp needle-like single crystals of PKU-1 were obtained with a yield of about 90% in Al (see the photograph of single crystals in Figure S1 in the Supporting Information).

Synthesis of Cr-Incorporated PKU-1 and PKU-5. The syntheses of PKU-1:*x*Cr^{3+} (x = 0.04−0.50) were carried out by adding an appropriate amount of $Cr(NO_3)_3\cdot 9H_2O$ by a similar method introduced above. The as-synthesized products are small needle crystals and show a gradual color change from colorless to green with increasing concentration of Cr^{3+} (see Figure S2 in the Supporting Information). PKU-5:*x*Cr^{3+} was prepared by heating the as-synthesized PKU-1:*x*Cr^{3+} at 750 °C for 10 h. The products show a gradual color change from white to purple with increasing concentration of Cr^{3+} (see Figure S3 in the Supporting Information). They were washed with water (25 °C) and treated ultrasonically to remove the excess boric oxide.

Structure Determination of PKU-1. A single crystal of PKU-1 in the size of about 0.30 mm × 0.03 mm × 0.03 mm was used for data collection on a Bruker SMART X-ray diffractometer equipped with an APEX-CCD area detector and using graphite-monochromized Mo Kα radiation (λ = 0.710 73 Å) at 290 K. The crystal structure was solved by the direct method and refined by full-matrix least-squares refinement. The detailed crystallographic information is provided in Tables S1−S3 in the Supporting Information.

Characterization. Powder XRD data for PKU-1:*x*Cr^{3+} and their calcined products PKU-5:*x*Cr^{3+} were collected on a PANalytical X'pert Pro equipped with a PIXcel detector and Cu Kα radiation (λ = 1.5406 Å). The operating voltage and current are 40 kV and 40 mA, respectively. Le Bail and Rietveld refinements were performed using the TOPAS software package.[18] High-quality XRD data for PKU-1:0.32Cr^{3+} were collected using monochromized Cu Kα1 radiation.

In situ high-temperature powder XRD experiments were carried out on a Bruker Advance D8 diffractometer (Cu Kα radiation) with a computer-controlled furnace. The sample was loaded on a platinum strip and heated from room temperature to 1200 °C in vacuum at a

dx.doi.org/10.1021/ic500352g | Inorg. Chem. 2014, 53, 5600−5608

heating rate of 5 °C/min, and the XRD data were collected after the temperature was stabilized for 1 h at every chosen temperature. Combined thermogravimetric (TG) and differential scanning calorimeter (DSC) analyses for PKU-1:xCr^{3+} (x = 0–0.50) were performed on a Mettler-Toledo TGA/DSC1 instrument at a heating rate of 10 °C/min from room temperature to 900 °C under N_2 flow. The doping content of Cr^{3+} for as-synthesized PKU-1:xCr^{3+} samples were analyzed by inductively coupled plasma-atomic emission spectrometry (ICP-AES) on a Leeman Profile-Spec. Transmission electron microscopy (TEM) images were taken using a JEM-2100F transmission electron microscope at an accelerating voltage of 200 kV. The ^{27}Al 3Q-MAS NMR spectrum was acquired on a Varian Infinity Plus spectrometer.

RESULTS AND DISCUSSION

Crystal Growth and Structure Redetermination of PKU-1. Polycrystalline PKU-1 was previously synthesized by direct reaction of $AlCl_3·6H_2O$ (Al_2O_3 or $Al(NO_3)_3·9H_2O$) with an excess of H_3BO_3 at 240 °C in a sealed autoclave. We speculated that an additional amount of water in boric acid flux system could reduce the viscosity of the flux and enhance the ion solubility and mobility. However, only small single crystals could be obtained by adding additional water. Eventually, we used an appropriate amount of concentrated HNO_3 aqueous solution instead of H_2O. The inner pressure could be further increased since the HNO_3 would decompose into gaseous NO_2. Brown gas came out when the autoclave was unsealed after the reaction. For a single-crystal growth, the heating rate was set to slow, and the reaction temperature was decreased to 220 °C. It should be mentioned that the added HNO_3 should be around 0.5 mL (in a 25 mL Teflon container); otherwise, either the crystals would be too small (if adding 0.25 mL of HNO_3 solution) or the yield would be low (if adding 1 mL of HNO_3 solution)

A structure reinvestigation for PKU-1 was conducted by single-crystal XRD. The previously reported structre was solved by powder XRD and is in the centrosymmetric space group $R\bar{3}$. The present data reveals that PKU-1 crystallizes in the trigonal space group $R3$ instead of $R\bar{3}$. An asymmetric structural fragment of PKU-1 is given in Figure S4 in the Supporting Information, and the structure projection along the c-axis is shown in Figure 1. The redetermined structure is topologically the same as the previous one but with a lower symmetry. As a consequence, there are three independent Al atoms, named Al1, Al2, and Al3. ^{27}Al 3Q-MAS NMR spectra support that

Table 1. Elemental Analyses by ICP-AES Method for Selected PKU-1:xCr^{3+} Samples

initial loading ratio	concentration from ICP-AES	calculated relative ratio
molar ratio (Cr/Al)	mg/L (Cr/Al)	molar ratio (Cr/Al)
0.12:0.88	2.67:11.27	0.109:0.891
0.20:0.80	6.97:13.33	0.213:0.787
0.36:0.64	10.09:9.64	0.352:0.648
0.50:0.50	10.0:5.40	0.490:0.510

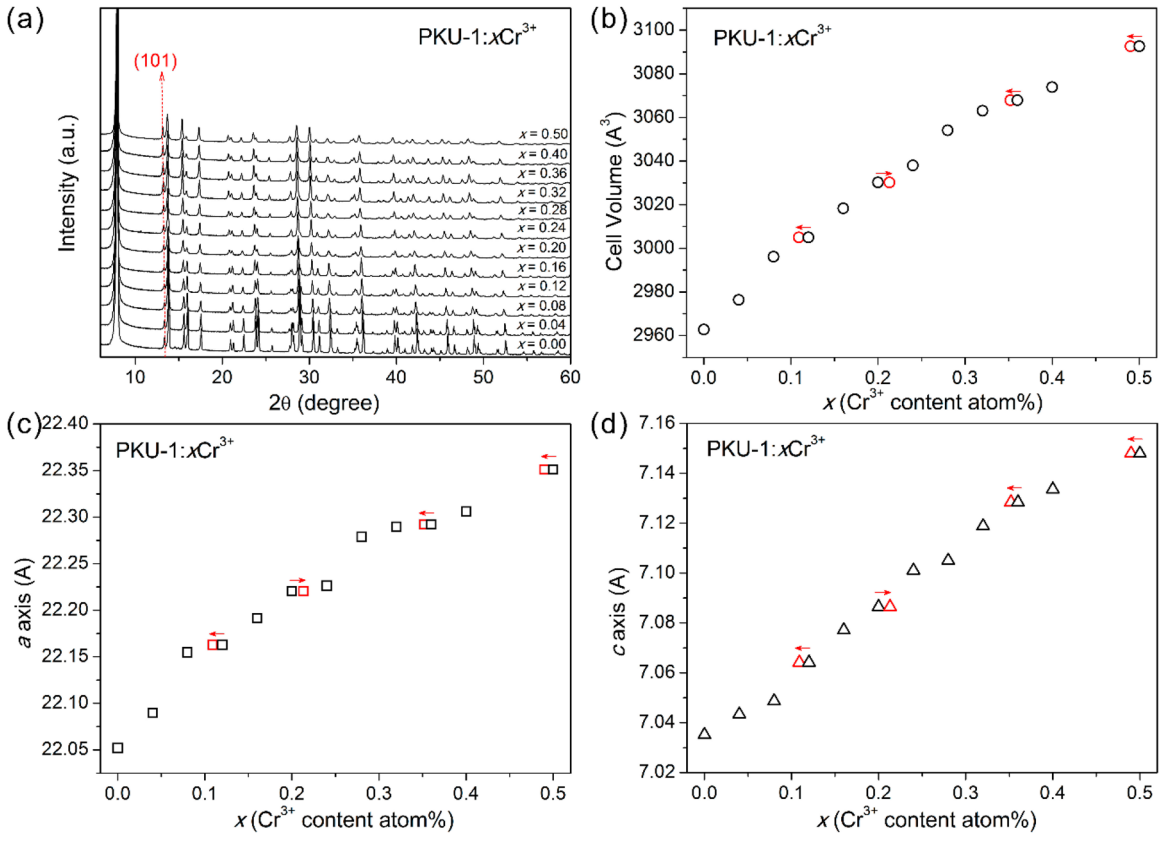

Figure 2. (a) Powder XRD patterns for PKU-1:xCr^{3+} samples. The reflection with the indices (101) shows a left-shift with increasing concentration of Cr^{3+}, indicating the cell lattice expansion. The exact cell lattice parameters, including cell volume and a- and c-axes are obtained by Le Bail fitting as shown in (b), (c), and (d), respectively. The red dots represent the calculated x values from ICP-AES experiments, which are close to the initial values.

dx.doi.org/10.1021/ic500352g | Inorg. Chem. 2014, 53, 5600–5608

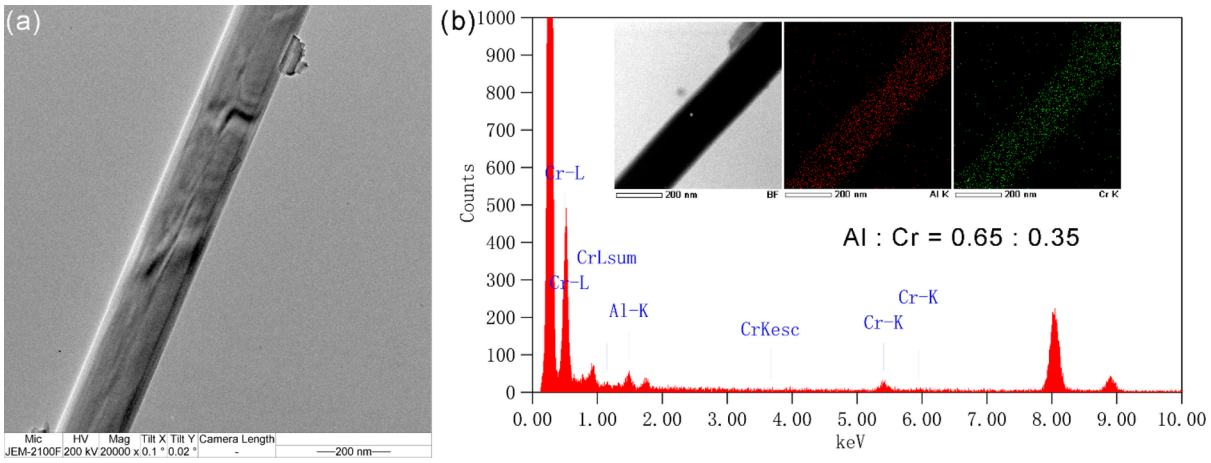

Figure 3. (a) TEM image of PKU-1:0.40Cr^{3+}. (b) Elemental analysis of as-prepared PKU-1:0.40Cr^{3+} by energy dispersive spectroscopy (EDS). (inset) The Cr/Al distribution map.

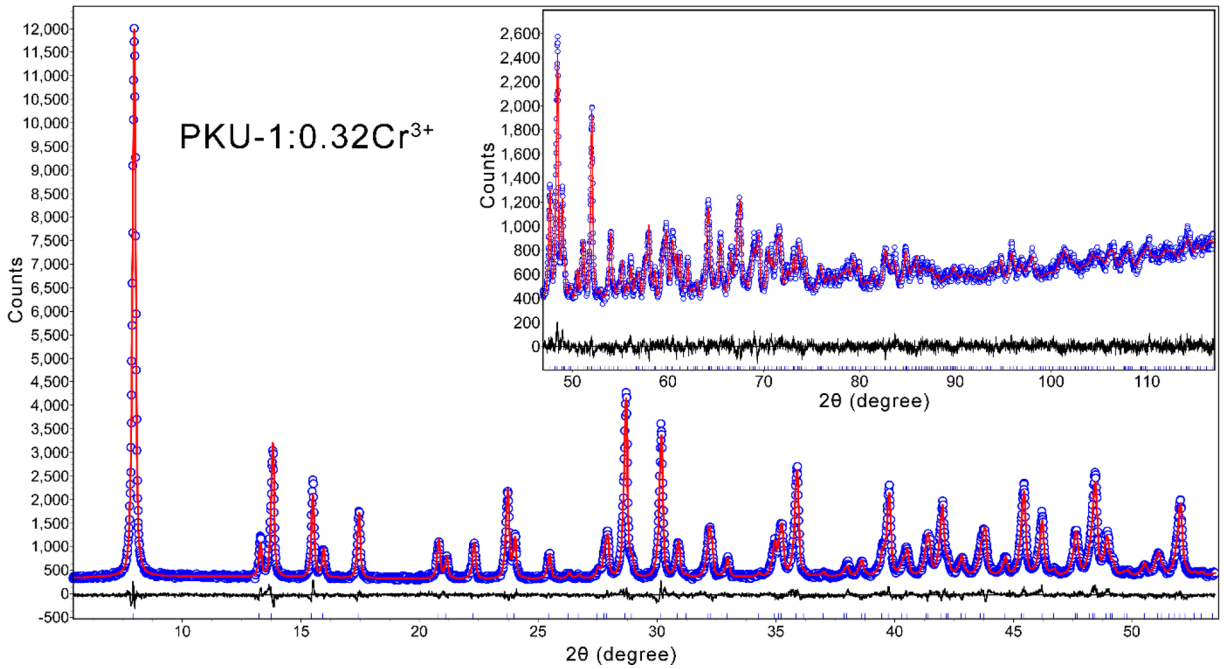

Figure 4. Final convergence of Retveld refinements for the PKU-1:0.32Cr^{3+} sample. The circles O and red solid line represent the observed and calculated patterns, respectively. The difference curve (in black) is also shown below the diffraction curves. (inset) Enlargement of the high-angle region.

there are three different Al sites (see Figure S5 in the Supporting Information). As highlighted in Figure 1, each $Al1O_6$ (or its topologically related $Al2O_6$) octahedron shares two edges with two other $Al1O_6$ (or $Al2O_6$) octahedra above and below to form a right-hand (or left-hand) helical octahedral chain along the *c*-axis. Those helix chains are further connected by $Al3O_6$ octahedra in a so-called trans-type connection to afford a three-dimensional framework. Clearly, borate ions are in the forms of BO_3 and B_2O_5 motifs. On the basis of bond-valence-sum calculations, it is assumed that five terminal oxygen atoms (O11, O12, O13, O14, and O15), which point to the channels, are protonated. So $BO(OH)_2$, $BO_2(OH)$, and $B_2O_4(OH)$ attach to the AlO_6-based framework by sharing vertex oxygen and form a neutral framework with the formula of $Al_3B_6O_{11}(OH)_5$.

The major cause of the lowering of the symmetry is the distortion of $Al3O_6$ octahedra. PKU-1 has a unique structure with large open space, and the three-dimensional framework is constructed exclusively of edge-shared octahedra; thus, the octahedra, which bond to rigid BO_3 and B_2O_5 motifs, need to afford strong static stress. Consequently, $Al3O_6$ is strongly distorted with five short (1.812(3)−1.869(3) Å; Table S3, Supporting Information) and one long (2.218(3) Å; Table S3, Supporting Information) Al−O bonds. This elongation of the Al3−O13 bond, on the other hand, can be viewed as a displacement (∼0.24 Å) of Al3 from its ideal position (see Figure S6 in the Supporting Information), which is the inversion center in the previous $R\bar{3}$ structure model. While Al1 and Al2 both have regular Al−O bond lengths (1.827(3)−1.959(3) Å; Table S3, Supporting Information). This deviation of Al3 atom from its hypothetical special position is the cause of the symmetry lowering of the framework.

Some of the extra-framework atoms were found to be in a triangular geometry and then refined as BO_3. Since the

dx.doi.org/10.1021/ic500352g | Inorg. Chem. 2014, 53, 5600−5608

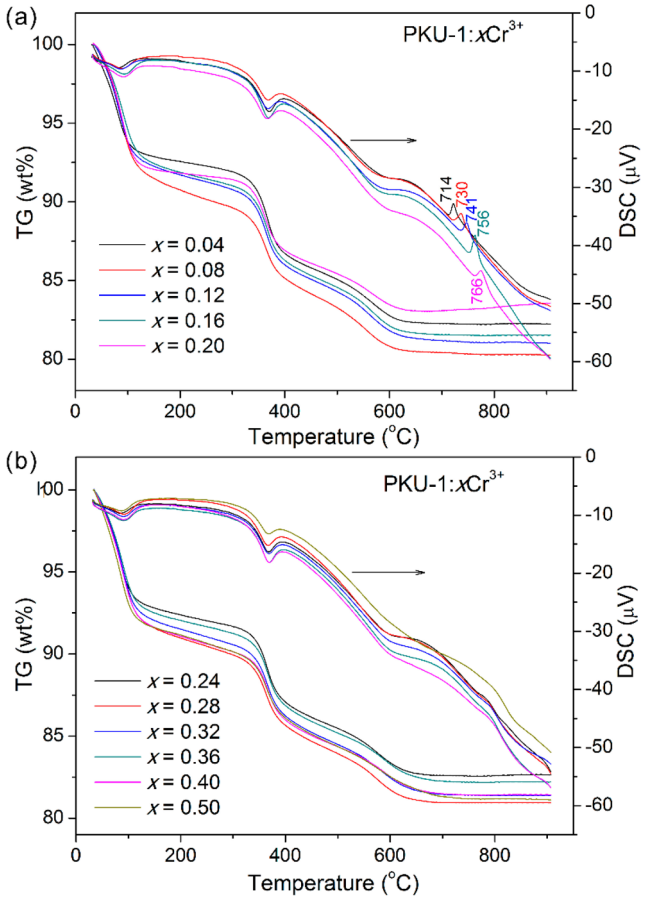

Figure 5. TG-DSC curves for PKU-1:xCr^{3+} (a) $x \leq 0.20$; (b) $0.24 \leq x \leq 0.50$.

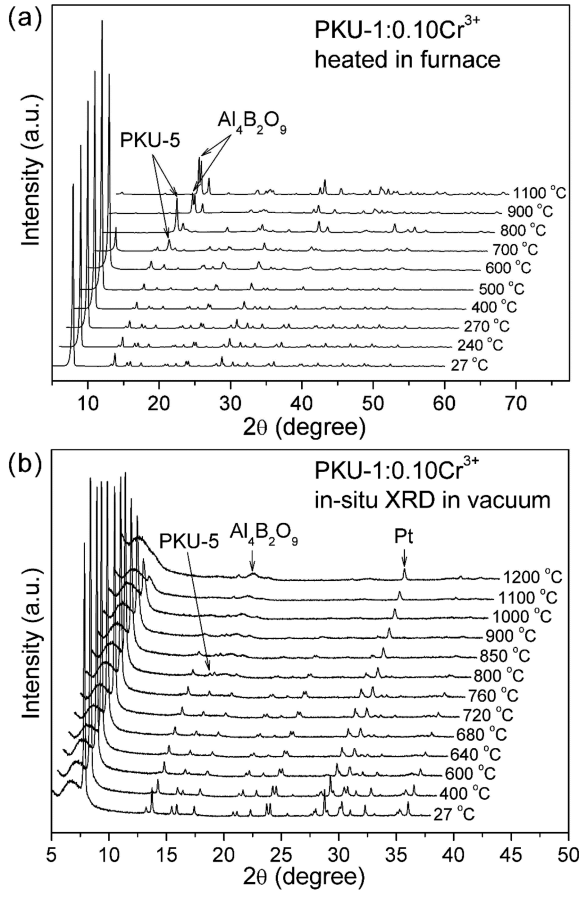

Figure 6. (a) XRD patterns of PKU-1:0.10Cr^{3+} sample heated at different temperatures in furnace. The PKU-5 phase appears at 700 °C and becomes the major phase at 800 °C, above which $Al_4B_2O_9$ is the thermally stable phase; (b) in situ XRD patterns in vacuum. The characteristic peak of PKU-1 phase at ~8° is still visible even at temperatures as high as 1000 °C.

framework is neutral, these BO_3 species were protonated as H_3BO_3. However, the size of H_3BO_3 does not exactly match the large open space of structural channels; consequently, there are no direct efficient hydrogen bonds between these H_3BO_3 and the framework. We believe that an additional amount of disordered water molecules are highly dispersed inside the channels, and behave as linkers between H_3BO_3 and the framework. TGA shows a three-step loss of weight (see Figure S7 in the Supporting Information). The weight loss below 200 °C (~11.5 wt %) originates from the evaporation of extra-framework water molecules and dehydration of H_3BO_3 as well. The calculated formula of PKU-1 is close to $Al_3B_6O_{11}(OH)_5 \cdot 2/3H_3BO_3 \cdot 2H_2O$. The exact amount of extra-framework molecules may be influenced by synthetic conditions and differ from sample to sample.

Cr^{3+}-Doping and Structure Analysis of PKU-1:xCr^{3+}. For Cr^{3+} substitution, $Al(NO_3)_3 \cdot 9H_2O$ and $Cr(NO_3)_3 \cdot 9H_2O$ were first dissolved in 0.5 mL of HNO_3 to form a homogeneous solution, and then boric acid was added. Apparently, this prereaction is efficient for the final synthesis of homogeneous Cr^{3+}-substituted samples. The doping content of Cr^{3+} was as high as ~50 atom % (discussed later), compared to 20 atom % in literature.[6] It is known that the substitution contents of the final products may not be exactly the same as the initial loading ratio, so elemental analyses were performed on four selected as-synthesized PKU-1:xCr^{3+} samples (see Table 1). The doping contents of Cr^{3+} (the values of x) determined by ICP-AES are close to the starting ratios of Cr/(Cr + Al); therefore, we used the initial x in the following part for convenience.

Powder XRD were performed on all as-synthesized PKU-1:xCr^{3+} samples, as shown in Figure 2a. The patterns are generally the same, and the reflection peaks, such as the (101) reflection, shifts to lower angles as x increases. The cell lattice parameters, including a, c, and V, were refined by Le Bail fitting (see Table S4 in the Supporting Information) and plotted in Figure 2b–d. We used the initial loading content of Cr^{3+} as x. We also used the x values from ICP-AES experiments (shown as red dots), which are close to the original x values. It is very clear that the cell lattice monotonously expands with Cr^{3+} substitution, which is not surprising due to the increase in ionic radii from Al^{3+} (0.535 Å) to Cr^{3+} (0.615 Å). The observation of a gradual change in color from white to green for PKU-1:xCr^{3+} ($0 \leq x \leq 0.50$) also supports the successful incorporation of Cr^{3+} (Figure S2, Supporting Information). Additionally, a TEM image was taken of the PKU-1:0.40Cr^{3+} sample showing a needle morphology, and the elemental analyses suggest the homogeneous distribution of Al^{3+} and Cr^{3+} all over the sample (see Figure 3).

High-quality powder XRD data were collected for a selected sample of PKU-1:0.32Cr^{3+}, using monochromized Cu Kα1 radiation. We performed Rietveld refinements to understand the doping behavior of Cr^{3+} at an atomic level. The occupancies of all three Al atoms are refined as free. As shown in Figure 4, it gives a good convergence by using the $R3$ model, and all the

dx.doi.org/10.1021/ic500352g | Inorg. Chem. 2014, 53, 5600–5608

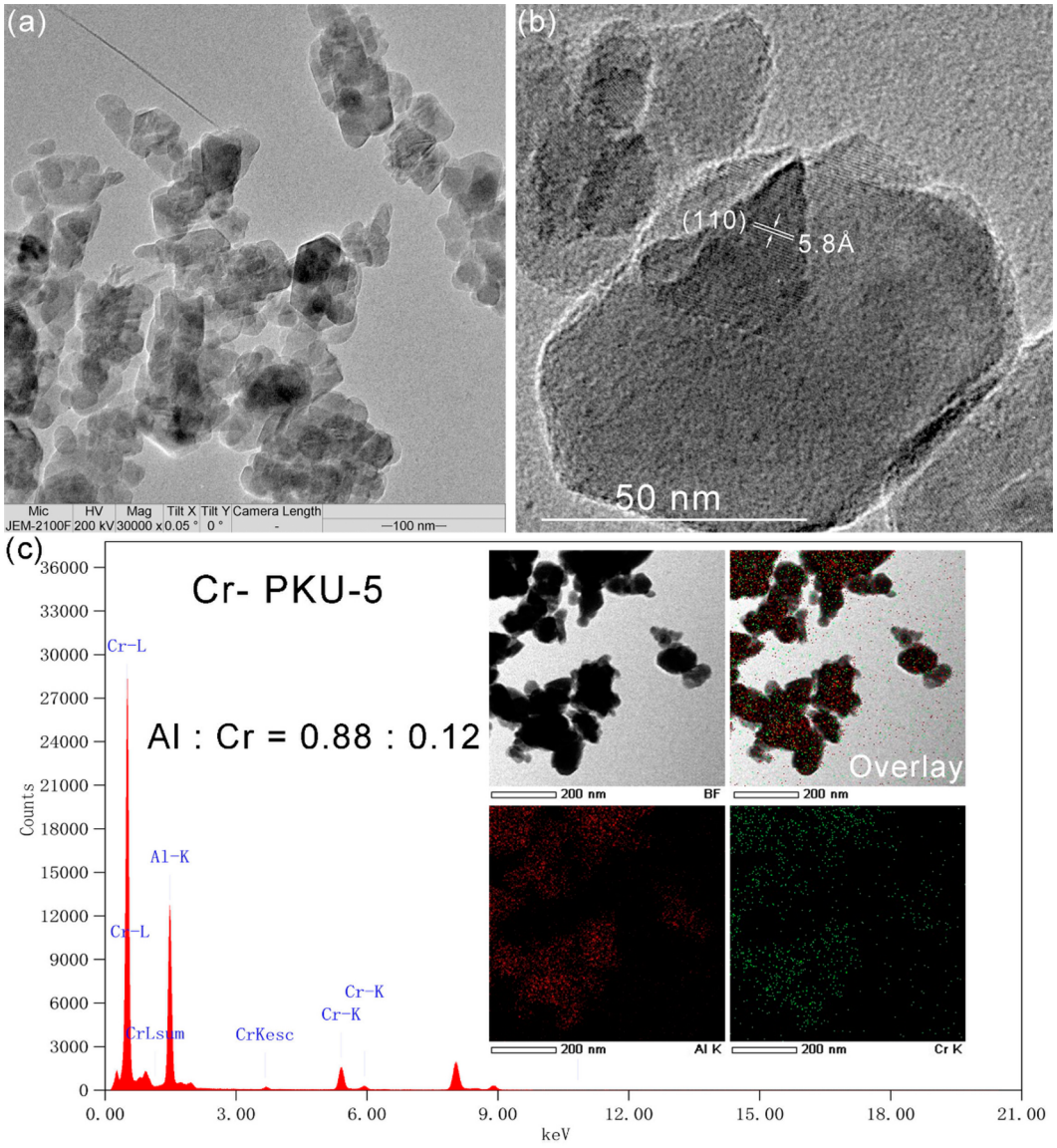

Figure 7. (a, b) TEM images for PKU-5:0.12Cr^{3+}. The spatial distance between stripes is ~5.8 Å, corresponding to the crystal planes with index value of {110}; (c) elemental analysis shows the Cr^{3+} concentration is 0.12. (inset) The Cr/Al distribution maps.

bond distances and angles are in the regular range. The final resultant parameters are given in Table S5 in the Supporting Information. We are particularly interested in the occupancies of the Al sites, which converge to 1.37, 1.20, and 1.09 for Al1, Al2, and Al3, respectively. First, the large (>1) occupancies consolidate the fact of successful substitution of heavy atoms on those sites. Second, it is suggested that Cr^{3+} prefers, statistically, to locate in the Al1 and Al2 sites rather than in the Al3 site. As discussed above, the Al3 locates at a strongly distorted environment with five short and one long metal−oxygen bonds. This cavity is probably not favored for Cr^{3+} with the $3d^3$ electron configuration.

Thermal Behavior of PKU-1:*x*Cr^{3+}. As precursors, hydrated polyborates could be calcined to prepare new anhydrous borates at elevated temperature. For example, PKU-5 with the formula of $Al_4B_6O_{15}$ was initially discovered during the thermal decomposition of PKU-1:*x*Cr^{3+}.[7]

Here we performed TG-DSC analyses for as-synthesized PKU-1:*x*Cr^{3+} (x = 0−0.50) samples at a heating rate of 10 °C/min under N_2 atmosphere. As shown in Figure 5, the thermal behaviors are quite similar, including the three steps of weight loss for dehydration from ~30 to 700 °C in the TG curves. These data can be interpreted according to those of undoped aluminoborate PKU-1, and the values of the three weight losses are summarized in Table S6 in the Supporting Information. It is apparent that the first three endothermic maxima in the DSC curves correspond to the dehydration processes. There is one distinct exothermic maximum for samples with $x \leq 0.20$ (Figure 5a). It should be noted that this exothermic maximum does not originate from the crystallization of PKU-5:*x*Cr^{3+} but from $Al_4B_2O_9$. We performed a powder XRD on the sample (x = 0.16) after heating to 775 °C in the DSC furnace. As shown in Figure S8 in the Supporting Information, it contains the diffraction peaks of $Al_4B_2O_9$ and H_3BO_3 (the appearance of H_3BO_3 is due to the water absorption by B_2O_3 in a moist environment). Additionally, there is a gradual increase of the exothermic maximum temperature from 714 to 766 °C when x increases from 0 to 0.20. When x is beyond 0.20, this exothermic maximum becomes diffused and hard to distinguish.

dx.doi.org/10.1021/ic500352g | Inorg. Chem. 2014, 53, 5600−5608

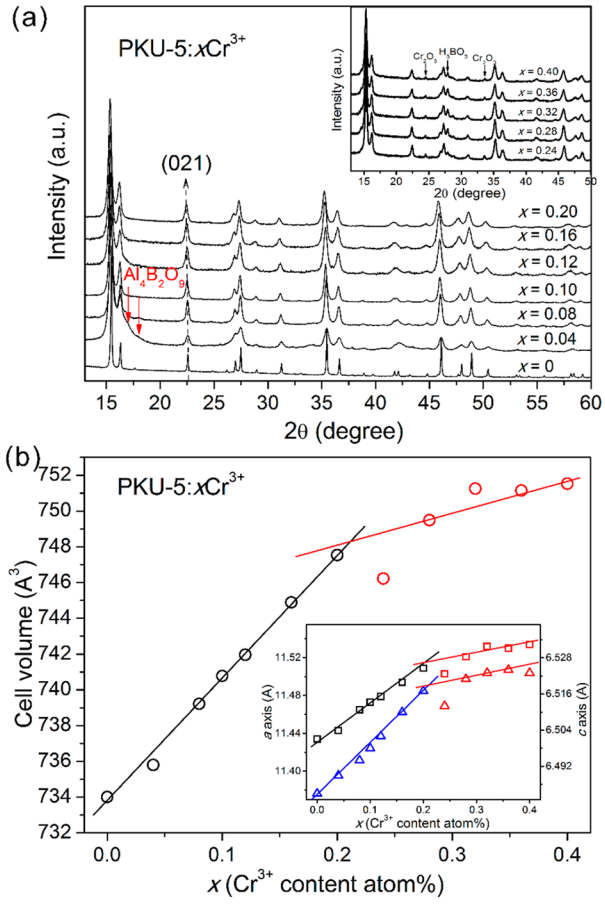

Figure 8. (a) Powder XRD patterns for PKU-5:xCr^{3+} samples. The reflection with the index (021) shows a left shift with increasing concentration of Cr^{3+}, indicating the cell lattice expansion; (b) cell lattice parameters obtained by Le Bail fitting vs x. The expansion tendency after x > 0.2 apparently slows down, which indicates the upper limit of Cr^{3+} concentration in PKU-5 is ~20 atom %.

The absence of PKU-5 during TG-DSC experiments is quite interesting. We speculate it is due to the very quick heating rate (10 °C/min), while the crystallization of PKU-5 probably needs a substantial period of time due to the kinetic effect. So we slowed down the DSC heating rate to 2 °C/min and obtained a light purple powder sample. According to powder XRD, PKU-5 becomes the major phase accompanied by $Al_4B_2O_9$ and H_3BO_3 (see Figure S9 in the Supporting Information).

To exclude the influence of the kinetic effect, prolonged annealing treatments on PKU-1:0.10Cr^{3+} in a muffle furnace at different temperatures were performed (5 h at each temperature), which were characterized by powder XRD (Figure 6a). The characteristic peak at ~8° (2θ) for PKU-1:0.10Cr^{3+} was still visible after annealing at 700 °C. At this temperature, the characteristic peaks of PKU-5:0.10Cr^{3+} started to appear, and then became the major phase at 800 °C. By further elevating the annealing temperature to 900 and 1100 °C, PKU-5:0.10Cr^{3+} disappeared completely and transformed to $Al_4B_2O_9$:0.10Cr^{3+}. The annealing products showed a color change sequence from light green (PKU-1:0.10Cr^{3+}) to light purple (PKU-5:0.10Cr^{3+}) and then to green ($Al_4B_2O_9$:0.10Cr^{3+}).

In-situ high-temperature powder XRD studies on the PKU-1:0.10Cr^{3+} sample were also performed in vacuum. As shown in Figure 6b, it is very interesting that the characteristic (110) reflection of PKU-1 was still visible after heated at 1100 °C (for 1 h), and the coexistence of PKU-1, PKU-5, and $Al_4B_2O_9$ was observed from 800 to 1000 °C, probably due to the short stabilization time for each temperature (1 h). Anyway, we believe that the vacuum condition is beneficial to stabilize the PKU-1 main framework.

Preparation and XRD Studies for PKU-5:xCr^{3+}. On the basis of the analyses of thermal behaviors for PKU-1:xCr^{3+}, we prepared PKU-5:xCr^{3+} powder by annealing PKU-1:xCr^{3+} at 750 °C for 10 h in a furnace. The byproduct B_2O_3 was washed by deionized water under ultrasonic conditions. The final resultant samples are nanoscaled bricklike particles with distinct facets, and the average particle size is about 30−60 nm in diameter (see Figure 7a). As shown in Figure 7b, the PKU-5 nanoparticles are well-crystallized, as indicated by the stripes belonging to the {110} crystal planes. A selected sample with x = 0.12 was analyzed by elemental mapping, indicating the well and homogeneous distribution of Cr^{3+} in the PKU-5 structure (see Figure 7c).

XRD patterns were collected for all annealing products, as shown in Figure 8a. The undoped PKU-5 is obtained from hydrothermal synthesis and shows particularly sharp peaks, while the peaks for PKU-5:xCr^{3+} are broad. When Cr^{3+} concentration is low ($x \leq 0.04$), it is hard to get pure PKU-5:xCr^{3+} phase, as it contains a small amount of $Al_4B_2O_9$ impurity (see Figure 8a). For $x \leq 0.20$, the reflection peak with the index of (021) shows a left shift, indicating the expansion of the cell lattice. Indeed, the refined cell parameters from Le Bail fitting increases along with Cr^{3+} content (see Supporting Information, Table S7 and Figure 8b). However, when x > 0.20, we cannot get pure PKU-5 phase but PKU-5 with a substantial amount of Cr_2O_3 (see the inset of Figure 8a). The increasing tendency of the refined cell parameters apparently slows down. We speculate that the upper limit of Cr^{3+} substitution into PKU-5 framework is ~20 atom %.

A representative sample of PKU-5:0.16Cr^{3+} was selected for Rietveld refinements (see Figure 9). There are two crystallographically independent aluminum atoms. Each AlO_6 octahedron shares three edges with neighboring octahedra, forming 10-membered channels. The framework of the PKU-5 carries a highly negative charge, and borate groups B_2O_5 are essential to compensate the negative charge by sharing common oxygen with AlO_6. The Rietveld refinement gives a good convergence (see Supporting Information, Table S8 for detailed refined parameters). However, we could not get a conclusive result of the site preference for Cr^{3+} substitution, because the Al1 and Al2 sites have almost the same occupancy parameter. It is probably due to the poor crystallization of PKU-5 sample obtained by thermal decomposition, or the low Cr^{3+} concentration in the structure. It is also possible that Cr^{3+} has no site preference in PKU-5 structure, unlike the case in PKU-1.

CONCLUSION

A structural redetermination of PKU-1 was performed by single-crystal XRD, and a symmetry lowering to $R3$ was observed. Among the three independent Al atoms, Al3 locates in a quite distorted octahedral environment, which releases the strong static stress of the main framework. A series of Cr^{3+}-substituted PKU-1 samples were successfully prepared and characterized by powder XRD, TEM, and TG-DSC. A very high Cr^{3+}-to-Al^{3+} substitution content in PKU-1 (~50 atom %) was achieved. Additionally, site-preference of Cr^{3+} substitution

dx.doi.org/10.1021/ic500352g | Inorg. Chem. 2014, 53, 5600−5608

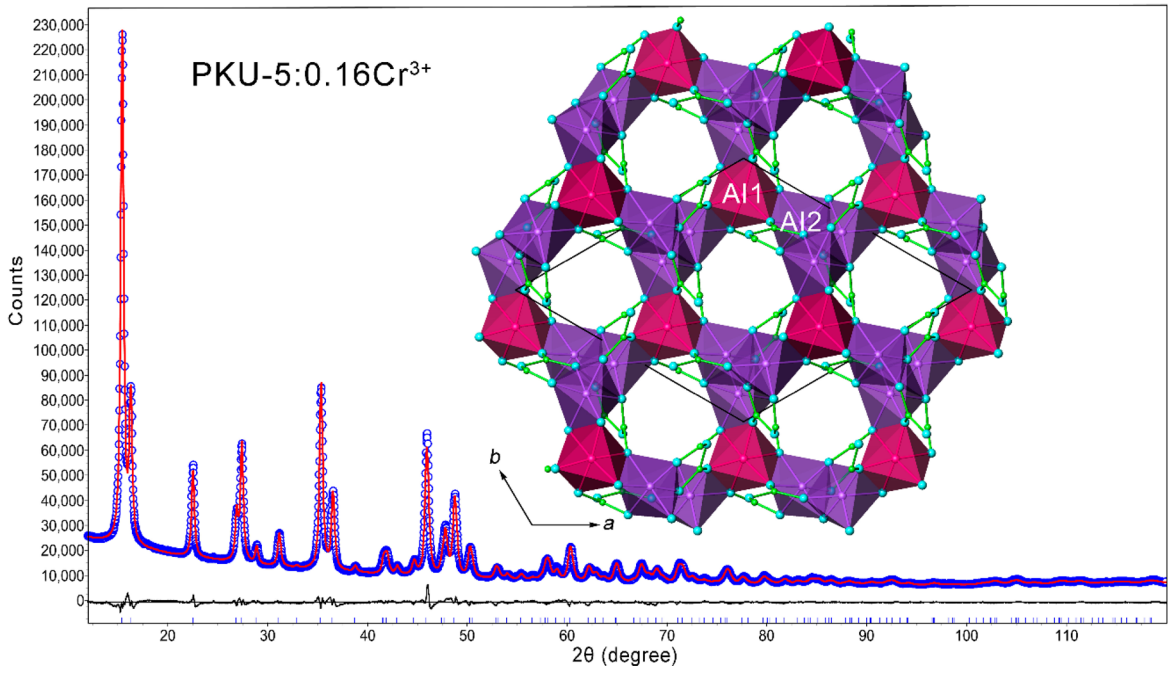

Figure 9. Final convergence of Retvield refinements on the PKU-5:0.16Cr^{3+} sample. The circles ○ and red solid line represent the observed and calculated pattern, respectively. The difference curve (in black) is also shown below the diffraction curves. (inset) The refined structure model of PKU-5, which contains two crystallographically independent Al atoms.

to Al1 and Al2 sites was observed by Rietveld refinements on PKU-1:0.32Cr^{3+} powder XRD. By Cr^{3+} substitution, the main framework of PKU-1 could be partially retained at 1100 °C in vacuum. When $0.04 \leq x \leq 0.20$, PKU-1:$x$$Cr^{3+}$ transformed to the PKU-5 structure at ∼750 °C by a 5 h annealing in air. For $x > 0.20$ in PKU-1:$x$$Cr^{3+}$, the heat treatment would lead to a composite of Cr^{3+}-substituted PKU-5 and Cr_2O_3, so the doping upper limit of Cr^{3+} in PKU-5 structure is around 20 atom %. Anyway, it is as expected that the Cr^{3+}-substitution contents into octahedra-based microporous borates are both quite high. Further investigations of the catalytic properties are in progress.

■ ASSOCIATED CONTENT

Supporting Information

Crystal structure in CIF format, atomic coordinates and selected bond distances for PKU-1; Rievteld refinement results for PKU-1:0.32Cr^{3+} and PKU-5:0.16Cr^{3+}; weight losses, cell parameters from Le Bail fitting for PKU-1:$x$$Cr^{3+}$ ($0.04 \leq x \leq 0.50$); cell parameters for PKU-5:$x$$Cr^{3+}$ ($0.04 \leq x \leq 0.50$); photographs for single crystals of PKU-1, as-synthesized PKU-1:$x$$Cr^{3+}$ and PKU-5:$x$$Cr^{3+}$ powder; asymmetric structural fragment of PKU-1; scheme of distortion from $R\bar{3}$ symmetry; ^{27}Al 3Q MAS NMR and TG-DTA for PKU-1; XRD for annealed samples in DSC furnace. This material is available free of charge via the Internet at http://pubs.acs.org.

■ AUTHOR INFORMATION

Corresponding Authors

*E-mail: taoyang@cqu.edu.cn. (T.Y.)
*E-mail: congrihong@cqu.edu.cn. (R.C.)

Notes

The authors declare no competing financial interest.

■ ACKNOWLEDGMENTS

This work was supported by the Nature Science Foundation of China (Grants 91222106, 21101175, 21171178, 21201012). Financial support from the Natural Science Foundation Project of Chongqing (CSTC 2012jjA0438) is also acknowledged.

■ REFERENCES

(1) Turner, S.; Buseck, P. R. *Science* **1981**, *212*, 1024−1027.
(2) Burns, R. G.; Burns, V. M.; Stockman, H. W. *Am. Mineral.* **1983**, *68*, 972−980.
(3) Shen, Y. F.; Zerger, R. P.; DeGuzman, R. N.; Suib, S. L.; McCurdy, L.; Potter, D. I.; O'Young, C. L. *Science* **1993**, *260*, 511−515.
(4) Murdoch, J. *Am. Mineral.* **1962**, *47*, 718.
(5) Guillou, N.; Gao, Q.; Forster, P. M.; Chang, J. S.; Nogues, M.; Park, S. E.; Férey, G.; Cheetham, A. K. *Angew. Chem., Int. Ed.* **2001**, *40*, 2831−2834.
(6) Ju, J.; Lin, J. H.; Li, G. B.; Yang, T.; Li, H. M.; Liao, F. H.; Loong, C. K.; You, L. P. *Angew. Chem., Int. Ed.* **2003**, *42*, 5607−5610.
(7) Ju, J.; Yang, T.; Li, G. B.; Liao, F. H.; Wang, Y. X.; You, L. P.; Lin, J. H. *Chem.—Eur. J.* **2004**, *10*, 3901−3906.
(8) Yang, T.; Bartoszewicz, A.; Ju, J.; Sun, J. L.; Liu, Z.; Zou, X. D.; Wang, Y. X.; Li, G. B.; Liao, F. .H.; Martín-Matute, B.; Lin, J. H. *Angew. Chem., Int. Ed.* **2011**, *123*, 12763−12766.
(9) Wang, G. M.; Li, J. H.; Huang, H. L.; Li, H.; Zhang, J. *Inorg. Chem.* **2008**, *47*, 5039−5041.
(10) Wang, G. M.; Li, J. H.; Li, Z. X.; Huang, H. L.; Xue, S. Y.; Liu, H. L. *Inorg. Chem.* **2008**, *47*, 1270−1272.
(11) Yang, S. H.; Li, G. B.; Ju, J.; Yang, Z. L.; Liao, F. H.; Wang, Y. X.; Lin, J. H. *Inorg. Chim. Acta* **2008**, *361*, 2413−2417.
(12) Yang, T.; Sun, J. L.; Eriksson, L.; Li, G. B.; Zou, X. D.; Liao, F. H.; Lin, J. H. *Inorg. Chem.* **2008**, *47*, 3228−3233.
(13) Zhou, J.; Zheng, S. T.; Zhang, M. Y.; Liu, G. Z.; Yang, G. Y. *CrystEngComm* **2009**, *11*, 2597−2600.
(14) Zhou, J.; Fang, W. H.; Rong, C.; Yang, G. Y. *Chem.—Eur. J.* **2010**, *16*, 4852−4863.
(15) Cheng, L.; Yang, G. Y. *Chem. Commun.* **2014**, *50*, 344−346.

(16) Guan, Y. J.; Zhang, D. M.; Wang, Y. M. *Catal. Lett.* **2012**, *142*, 1225−1233.
(17) Gao, W. L.; Yang, T.; Wang, Y. X.; Li, G. B.; Liao, F. H.; Lin, J. H. *J. Phys. Chem. B* **2005**, *109*, 22775−22779.
(18) *TOPAS, V4.1-beta;* Bruker AXS: Karlsruhe, Germany, 2004.